

INTERNATIONAL SOCIETY FOR SOIL MECHANICS AND GEOTECHNICAL ENGINEERING



This paper was downloaded from the Online Library of the International Society for Soil Mechanics and Geotechnical Engineering (ISSMGE). The library is available here:

<https://www.issmge.org/publications/online-library>

This is an open-access database that archives thousands of papers published under the Auspices of the ISSMGE and maintained by the Innovation and Development Committee of ISSMGE.

The paper was published in the proceedings of the 7th International Symposium on Geotechnical Safety and Risk (ISGSR 2019) and was edited by Jianye Ching, Dian-Qing Li and Jie Zhang. The conference was held in Taipei, Taiwan 11-13 December 2019.

Interaction of Geotechnical and Structural Variabilities in Reliability Assessments of Retaining Walls

X. Chen¹, Y. F. Leung², and T. M. Chan³

¹Department of Civil and Environmental Engineering, The Hong Kong Polytechnic University, Hong Kong.

E-mail: xiaoyu19.chen@connect.polyu.hk

²Department of Civil and Environmental Engineering, The Hong Kong Polytechnic University, Hong Kong.

E-mail: andy.yf.leung@polyu.edu.hk

³Department of Civil and Environmental Engineering, The Hong Kong Polytechnic University, Hong Kong.

E-mail: tak-ming.chan@polyu.edu.hk

Abstract: This paper presents the reliability assessment for three types of retaining walls, including deep cement mixing (DCM) retaining wall and reinforced DCM wall, both embedded in soils, and DCM wall founded on stiff stratum, with the spatially variable soil and wall materials individually modeled by the random field theory. The random field realizations are generated by Latin hypercube sampling with dependence (LHSD), which is a stratified sampling technique that preserves the spatial autocorrelation characteristics of the materials. For each set of variability features, 1000 realizations are generated, and the subsequent analyses are performed in *FLAC3D*, with the numerical model verified by a series of mesh refinement studies. Both the spatially variable soil and wall materials are shown to significantly affect the system response, and their relative contributions are elucidated through the probabilistic analyses with different combinations of soil and wall property variations. The results show how the overall performance uncertainty may be affected by the types of retaining walls, and the variability in geotechnical and structural materials. Through these analyses, this paper aims to demonstrate the needs to consider both the geotechnical and structural variabilities in probabilistic analyses, and reappraise the performance discrepancies between these types of walls from the perspective of spatial variability in the materials.

Keywords: Retaining wall; soil-structure interaction; spatial variability; probabilistic analyses; random field modeling.

1 Introduction

The significance of geotechnical uncertainties on the performance of geotechnical systems has long been recognized (e.g., Phoon et al. 1999a, b; Baecher et al. 2003). Apart from geotechnical variability, characteristics of the structural system can also exert significant impacts on overall system performance. For retaining structures constructed by the deep cement mixing (DCM) technique, the wall material involves highly variable properties, with coefficient of variation (cov) ranging from 0.15 to 1.35 (Navin et al. 2005). Such variations in the wall materials may arise from the variability of in situ soils, mixing effectiveness and other factors. Misunderstanding or ignoring those variabilities can lead to substantial risks in projects, as this may cause oversight of certain mechanisms in the performance of the system.

This paper assesses the interaction effects between geotechnical and structural variabilities on the overall system stability, based on results of probabilistic analyses. The Young's modulus of the wall material and the soil are assumed to be spatially correlated, and are individually modeled by Latin hypercube sampling with dependence (LHSD). System responses of three different DCM wall configurations are compared in order to demonstrate the significance of holistic consideration of the geotechnical and structural spatial variabilities. The relative contributions of geotechnical and structural variabilities to the overall response are investigated, where the discrepancies between the three wall types are also discussed.

2 Mesh Refinement Study

To model the random field of wall properties, the retaining wall is modeled by solid elements in the *FLAC3D* software, which is a finite difference package. This is different from the usual practice of adopting 'structural elements' for deterministic analyses of retaining walls. The mesh quality is crucial in these solid element models, to ensure the stability, accuracy, and fast convergence of numerical simulations. It is necessary to adopt meshes that balance the computational demands and accuracy for the specific model configuration. Based on the parametric studies presented by Abbasi et al. (2013), brick elements with aspect ratio of 1:1 are preferred as they are associated with smaller errors and compare well with the analytical solutions. In this study, a series of mesh refinement analyses are performed to determine the required number of elements (or 'zones' as defined in the *FLAC3D* software) to accurately represent the retaining wall as solid elements under lateral loading.

Proceedings of the 7th International Symposium on Geotechnical Safety and Risk (ISGSR)

Editors: Jianye Ching, Dian-Qing Li and Jie Zhang

Copyright © ISGSR 2019 Editors. All rights reserved.

Published by Research Publishing, Singapore.

ISBN: 978-981-11-2725-0; doi:10.3850/978-981-11-2725-0_IS14-1-cd

2.1 Simple cantilever column

Figure 1(a) shows a cantilever column with length of 6 m, width of 1 m and thickness of 1 m, simulated by elastic solid elements in *FLAC3D* (without modeling soils). The Young's modulus of the column material, E , is 600 MPa with Poisson's ratio, ν , of 0.25. When the column is subjected to a lateral uniformly distributed pressure q_0 (4000N/m²), the maximum deflection, d_{\max} , can be determined analytically by Eq. (1):

$$d_{\max} = \frac{ql^4}{8EI} \quad (1)$$

where q ($= q_0 \times 1\text{m}$) is the line load, and is equal to 4000N/m in this study; l is the column length; and I is the second moment of area of the column in the direction of loading. The purpose of this numerical experiment is to test the number of zones required to accurately model an elastic structural column using solid elements, and the lateral pressure does not necessarily represent soil pressure, as soil is not simulated in this model.

The accuracy of *FLAC3D* models improves with finer meshes as shown in Figure 1(b). Keeping a 1:1 aspect ratio, six zones across the thickness of the column are adequate to represent the column performance under lateral uniform distributed loading.

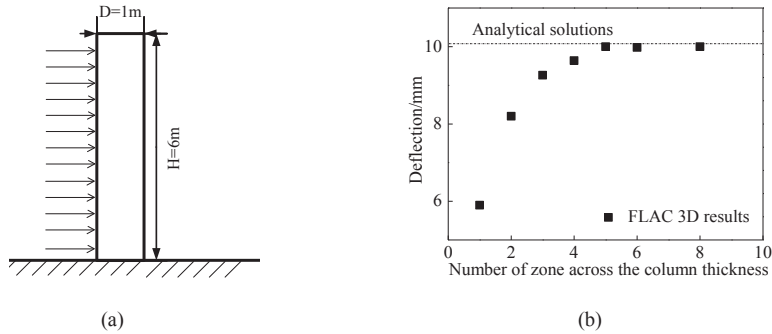


Figure 1. (a) Elevation view and (b) *FLAC3D* and analytical results of the cantilever column under lateral loads.

2.2 Retaining wall

A hypothetical retaining wall configuration (shown in Figure 2(a)) with wall material properties identical to the simple cantilever column is analyzed with *FLAC3D*, to demonstrate the applicability of mesh refinement results to retaining wall problems. The wall has a total length of 11 m and supports a 5-m excavation. The soil surrounding the wall is modeled as Mohr-Coulomb material with Young's modulus of 16 MPa, Poisson ratio of 0.3 and friction angle of 22°.

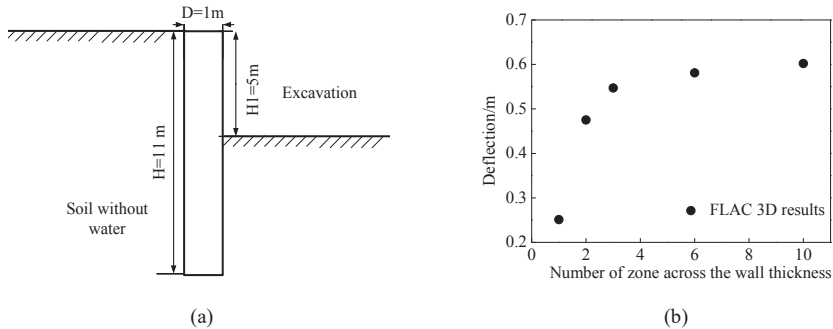


Figure 2. (a) Elevation view and (b) *FLAC3D* results of the hypothetical retaining wall.

The maximum wall deflections obtained by numerical models of different mesh densities are shown in Figure 2(b). Similar to the case of simple cantilever column, six zones across the wall thickness is enough to simulate the wall response, as further refinement does not lead to significant changes in the numerical results. This demonstrates the validity of mesh refinement when the wall structure is represented by solid elements, providing a basis for the modeling assumptions to balance between accuracy and computational demands.

3 DCM Retaining Walls: Problem Geometry, Model Parameters, and Modeling Approach

3.1 Problem geometry

Three hypothetical retaining walls, including deep cement mixing (DCM) retaining wall (Figure 3(a)), reinforced DCM retaining wall with steel H-pile reinforcement (Figure 3(b)), and DCM retaining wall (unreinforced) founded on stiff stratum (Figure 3(c)), are analyzed to illustrate the interactions between geotechnical and structural variabilities and their influence on the overall system response. The geometry of the reinforced DCM wall is identical to the study by Taki et al. (1991), with thickness (transverse direction) of 1.2 m and height of 11 m. In the *FLAC3D* model, a section of the wall is simulated, with a model width (longitudinal direction) of 1.5 m, which is a typical spacing between H-sections for the reinforced DCM wall. The unreinforced DCM walls (in soil and on stiff stratum) have similar geometries to the reinforced DCM retaining wall, except that their thickness is adjusted to 2.2 m, so that the three types of retaining walls have similar bending stiffness.

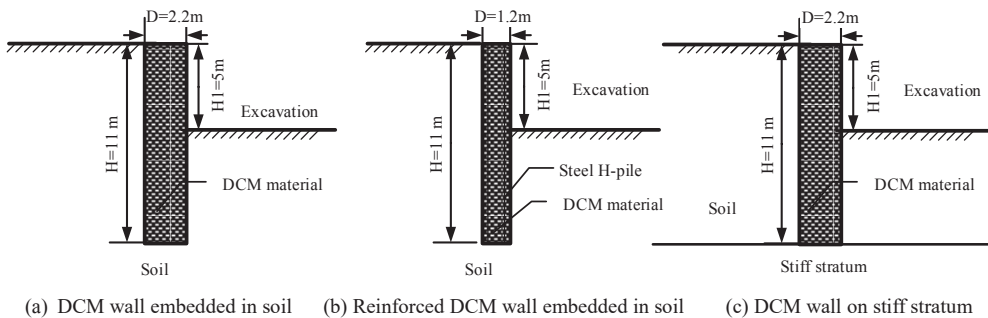


Figure 3. Geometries of the three types of retaining walls.

3.2 *FLAC3D* model conditions

The soil and retaining walls are modeled in *FLAC3D* by solid elements and are represented as Mohr-Coulomb material and elastic material, respectively, while the steel H-pile inside the reinforced DCM wall is simulated by shell elements. The friction angle of the soil is 33° with zero cohesion. Figure 3(c) is regarded as an extreme condition where the stratum below the retaining wall is very stiff, which is simulated by a fixed boundary. The material properties adopted in the numerical analyses are included in Table 1.

Table 1. Material properties adopted in the numerical analyses.

Material	Soil	DCM material	H pile inside reinforced DCM wall
Young's modulus E (kPa)	16×10^3	600×10^3	200×10^6
Poisson's ratio ν	0.3	0.25	0.3
Unit weight γ (kN/m ³)	18	21	-

To minimize boundary effects, the horizontal distance from wall to model boundaries is set at 3 times of the excavation depth, and the distance from wall toe to bottom of the model is equal to the excavation depth (Duncan and Goodman 1968). Roller boundaries are applied to the lateral boundaries of the model, and the bottom of the model is fixed in all directions. The maximum wall deflection is recoded in *FLAC3D* after the excavation process. The number of zones (solid elements) representing the wall is defined through the abovementioned mesh refinement study, and coarser elements are adopted in regions near the model boundaries, where the deflections and stress changes are small. The total numbers of zones are 9180, 26240, and 8670 for the *FLAC3D* models of DCM wall, reinforced DCM wall, and DCM wall on stiff stratum, respectively. Deterministic analyses for the three configurations are first performed with uniform soil and wall properties in *FLAC3D*. The corresponding maximum deflections of three types of walls are 40 mm, 35 mm, 13 mm.

3.3 Probabilistic analyses based on LHSD

In the probabilistic analyses of the current study, the Young's modulus E of the soil and wall materials are assumed to be lognormally distributed, and their variations are simulated by Latin hypercube sampling with dependence (LHSD) (Lo and Leung 2017). Properties of the steel H-pile inside the DCM wall (for the reinforced wall) are assumed to be uniform, since the variability in structural steel is normally insignificant compared to soils or soil-cement mixture. The mean Young's moduli of the soil (μ_{soil}) and DCM material (μ_{DCM}) are 16 MPa and 600 MPa, respectively, with cov of the soil as 0.25 or 0.5, and cov of the DCM material as 0.5 or 1 in

various analyses. The Poisson's ratio is constant and equals 0.3 for soil and 0.25 for DCM materials. To simplify the scenarios, probabilistic analyses are presented assuming that the soil and wall materials have isotropic correlation structures. In both horizontal and vertical directions, the autocorrelation distance is assigned to be 5 m for soil and 2 m for DCM materials. The influence of anisotropic spatial correlation will be briefly discussed in later sections. As the initial random field generated by LHSD is Gaussian distribution, transformation on lognormal distribution to Gaussian distribution is necessary. The mean and standard deviation of the soil and DCM materials are derived from cov_{soil} , cov_{DCM} , as follows:

$$\sigma_{\ln E} = \sqrt{\ln(1 + \text{cov}_E^2)}; \quad \mu_{\ln E} = \ln \mu_E - \frac{1}{2} \sigma_{\ln E}^2 \quad (2)$$

For both soil and DCM wall materials, the spatial correlation coefficient (ρ) is represented by a squared exponential function:

$$\rho(i, j) = \exp \left[- \left(\frac{\sqrt{(x_i - x_j)^2 + (y_i - y_j)^2}}{r_{xy}} \right)^2 - \left(\frac{|z_i - z_j|}{r_z} \right)^2 \right] \quad (3)$$

where $|x_i - x_j|$, $|y_i - y_j|$, $|z_i - z_j|$ are separation distances between i and j in x , y and z directions; r_{xy} , r_z are the lateral and vertical autocorrelation distances.

Figure 4 shows typical realizations of random fields of Young's modulus in *FLAC3D*. Figures 4(a) and (b) involve different color scales to illustrate the variations of properties in the two types of materials. In the subsequent discussions, 1000 realizations are generated, with the analyses automated in *FLAC3D* for each combination of wall/soil variability.

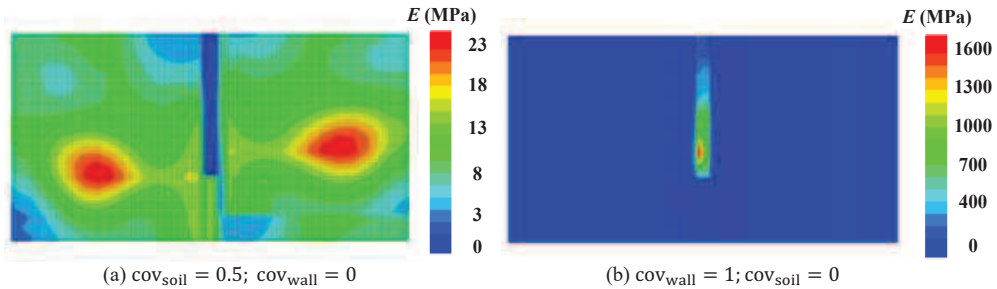


Figure 4. Typical realization of random fields of Young's modulus E .

4 Results and Discussions

To illustrate the significance of holistic considerations of geotechnical and structural variabilities, three series of analyses are performed: (a) probabilistic analyses with spatially variable soil only ($\text{cov}_{\text{soil}}=0.5$; $\text{cov}_{\text{wall}}=0$); (b) probabilistic analyses with spatially variable DCM materials only ($\text{cov}_{\text{soil}}=0$; $\text{cov}_{\text{DCM}}=1$); and (c) probabilistic analyses with high overall variability ($\text{cov}_{\text{soil}}=0.5$, $\text{cov}_{\text{DCM}}=1$) and low overall variability ($\text{cov}_{\text{soil}}=0.25$, $\text{cov}_{\text{DCM}}=0.5$) in both materials. Instead of comparing the magnitudes of wall deflections in the three wall types, this study focuses on the dimensionless wall deflection factor, F_d , to avoid the differences arising from retaining wall configurations. The factor is defined as $F_d = d_i / d_{\text{det}}$, where d_i is the maximum wall displacement from the i^{th} realization and d_{det} is the maximum wall deflection from deterministic analysis.

4.1 Effects of soil and wall spatial variability

Figure 5 shows the probability density function (PDF) of wall deflection factor of three types of retaining walls, obtained by probabilistic analyses under the three different conditions of soil/wall variability. Compared to the other two conditions, probabilistic analysis with overall variation would result in a larger variance in the wall deflection factor, as shown by the relatively wide distribution, large mean and standard deviation value.

A closer examination reveals that the retaining wall types also significantly affect the system uncertainty. For reinforced DCM retaining wall, the variations of soil-cement material alone do not significantly affect the wall performance. This is because the steel H pile contributes more (than the soil-cement mixture) to the bending rigidity of the system, but steel involves little variability and is modeled as a uniform material. Consequently, the PDF is very close to the corresponding deterministic analysis when cov_{soil} is set as 0. That means the response

uncertainty of the reinforced wall is fundamentally governed by geotechnical variability.

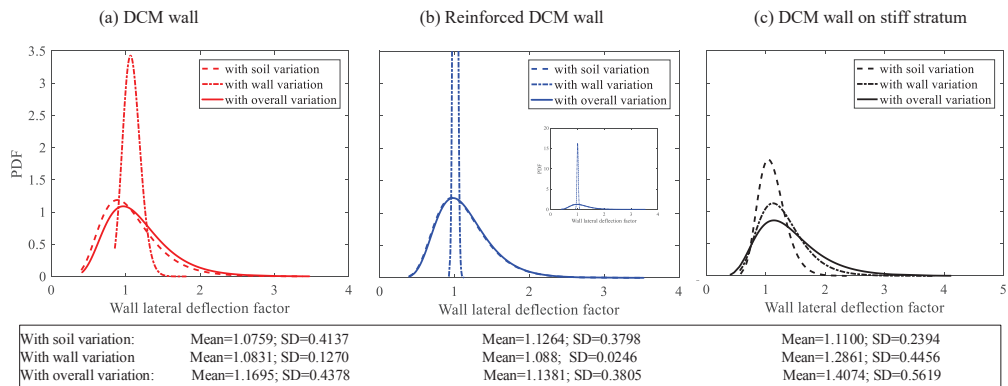


Figure 5. Probability density function for wall deflection factor with different soil and wall property variations combinations.

A different pattern is observed for the unreinforced DCM walls (wall embedded in soils and wall on stiff stratum). Both the geotechnical spatial feature and structural variability impact the overall performance of the unreinforced walls, but in a different way. In particular, the performance uncertainty of retaining wall on stiff layer is profoundly affected by variations in the wall material. As the structural element formed by DCM technique involves significant variations, ignoring these variations may lead to oversight of the hidden risks in the overall system performance.

The impacts of the overall variation (both soil and wall material variability) on the retaining wall response are then investigated for the three types of retaining walls. The PDF of wall lateral deflection factor under low overall variation ($\text{cov}_{\text{soil}}=0.25$, $\text{cov}_{\text{DCM}}=0.5$) and high overall variation ($\text{cov}_{\text{soil}}=0.5$, $\text{cov}_{\text{DCM}}=1$) are shown in Figure 6. The mean estimates of F_d are all larger than one, which indicates that spatially variable material property generally increases the lateral deflection of the retaining wall. With relatively small overall variations, the standard deviations are less than 21% of the deterministic estimates d_{det} . High overall variations in soil and wall materials lead to a larger variance in wall system response, where the standard deviations approach 56% of d_{det} . It is interesting to note that while the DCM wall on stiff stratum entails the smallest deterministic estimate of wall deflection (13 mm), it is in fact associated with the highest performance uncertainty as the variations in both the soil and wall materials contribute significantly.

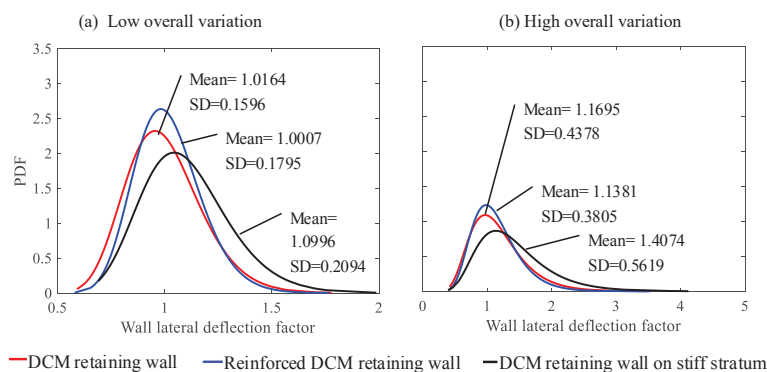


Figure 6. Probability density functions for wall deflection factor of three types of retaining walls.

4.2 Effects of autocorrelation distance and variability in shear strength of soil

Soil materials often involve cross-correlated strength and stiffness properties, and anisotropic spatial correlation features, manifested as different autocorrelation distances along various directions (e.g. Liu and Leung 2018). This study also performs preliminary investigations into these effects under the scenario of DCM retaining walls. Figure 7 shows the base case (in red line) of DCM retaining wall embedded in soils with isotropic

autocorrelation distance of 5 m, compared with the anisotropic spatial correlation (in blue line) with $r_{xy} = 50$ m and $r_z = 5$ m. In this case, the results are not significantly different, which may be attributed to the fact that the excavation depth is only 5 m. This means the ‘active’ zone behind the wall also extends to a horizontal distance in the order of about 5 m, and larger values of r_{xy} do not cause much difference in the probabilistic estimates. When cross-correlation between Young’s modulus and friction angle of the soil is considered (in black line; cross-correlation coefficient = 0.5), the performance uncertainty is increased, and the interactions with various wall type and wall material features may be investigated in a future parametric study.

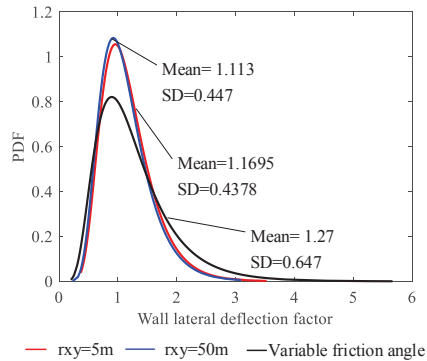


Figure 7. Probability density functions for wall deflection factor of three cases.

5 Conclusion

This paper assesses the interaction effects of geotechnical and structural variations and their impacts on the system response, through random field analyses of three types of retaining walls constructed by the DCM technique. The performance uncertainty of the reinforced DCM wall appears to be fundamentally governed by geotechnical variability, if the variability of structural steel reinforcement (H-section) can be considered insignificant. For unreinforced DCM walls embedded in soils or founded on stiff layer, apart from the geotechnical spatial features, the variability features of wall materials is also found to influence the system uncertainty. In particular, the performance uncertainty of DCM wall on stiff stratum is mainly controlled by variability in wall material, while the soil variability features contribute more when the wall is embedded in soils. It is important for practitioners to recognize the discrepancies between different types of walls, and consider the geotechnical and structural variabilities accordingly when performing reliability assessments.

Acknowledgments

The work presented in this paper is financially supported by the Research Grants Council of the Hong Kong Special Administrative Region (Project No. 15212418).

References

- Abbasi, B., Russell, D., and Taghavi, R. (2013). FLAC3D mesh and zone quality. *Proceedings of the 3rd International FLAC / DEM Symposium*, Itasca International Inc., Hangzhou, China.
- Duncan, J.M. and Goodman, R.E. (1968). *Finite Element Analyses of Slopes in Jointed Rock*, University of California, Berkeley, Office of Research Services.
- Liu, W.F. and Leung, Y.F. (2018). Characterising three-dimensional anisotropic spatial correlation of soil properties through in situ test results. *Geotechnique*, 68(9), 805-819.
- Lo, M.K. and Leung, Y.F. (2017). Probabilistic analyses of slopes and footings with spatially variable soils considering cross-correlation and conditioned random field. *Journal of Geotechnical and Geoenvironmental Engineering*, 143(9): 04017044.
- Navin, M.P. (2005). *Stability of Embankments Founded on Soft Soil Improved with Deep-Mixing-Method Columns*, PhD thesis, Virginia Polytechnic Institute and State University, Blacksburg, VA, USA.
- Phoon, K.K. and Kulhawy, F.H. (1999a). Characterization of geotechnical variability. *Canadian Geotechnical Journal*, 36(4), 612-624.
- Phoon, K.K. and Kulhawy F.H. (1999b). Evaluation of geotechnical property variability. *Canadian Geotechnical Journal*, 36(4), 625-639.
- Taki, O. and Yang, D.S. (1991). Soil-cement mixed wall technique. *Geotechnical Engineering Congress*, ASCE, Boulder, Special publication, 27, 298-309.